

much less opaque and often semitransparent in appearance, and (ii) much more resistant to drilling and sawing than first-year ice. These changes are attributed to the exposure of the ice to elevated temperature and solar radiation during the previous summer or summers, which not only results in substantial loss of brine, as borne out by salinity measurements, but also produces significant changes in the crystalline texture of the ice. These changes include major modification of the ice plate and brine lamella substructure of crystals, sometimes to the point of virtually complete obliteration of brine pockets, and substantial smoothing out of the typically angular, interpenetrated outlines of the crystals themselves. We term such textural modification as retexturing. An example of such structure and that of fresh, unmodified congelation ice is shown in Fig. 5, A and B. This retexturing, which was observed to depths of a meter or more, is probably equivalent to the so-called recrystallization inferred from microwave measurements (9) to have occurred in the upper levels of multiyear ice in the Beaufort Sea.

Retexturing of sea ice occurs simultaneously with flushing of summer surface melt water, which is the principal mechanism by which brine is drained downward from the floe to create ice with multiyear salinity characteristics. Ultimately the ice at the top of the floe, which is retextured, glacier-like, and brine-poor, bears little resemblance to the original sea ice. Such modification should result in significant changes in the mechanical and electromagnetic properties of this ice and in its response to remote-sensing signals.

Although drilling the top meter or so of floes generally sufficed to distinguish between first-year and multiyear ice types, complete drilling of a multiyear floe is needed to obtain an estimate of its age. Most floes show some evidence of aligned  $c$ -axis structure related to the growth of ice under the direct influence of currents at the growing ice interface (10). Alignment changes in a multiyear floe thus constitute a record of the orientation of the floe with respect to the direction of current motion directly beneath the ice. We assume that the alignment directions of the  $c$ -axes occur on an annually repeating basis, which is consistent with wintertime growth under conditions of an immobilized or tight pack. Such changes in alignment direction together with crystal size and shape changes and surges in the salinity profile (which often coincide with changes of crystal alignment) can be used to estimate the ages of multiyear floes. Floes demonstrably older than 4 to 5 years were not observed. Conversely, the absence of aligned  $c$ -axis structure can be correlated

most probably with growth during unencumbered drift or rotation of the ice floe with respect to the direction of the current directly beneath the ice. This was a common condition of recently formed or actively growing ice on the bottom of floes as they exited Fram Strait.

#### REFERENCES AND NOTES

1. T. E. Vinje, *Norsk Polarinstitutt Arbok* (1975).
2. V. T. Timofeyev, *Probl. Arktiki Antarkt.* 5, 27 (1958); K. Aagaard and P. Greisman, *J. Geophys. Res.* 80, 3821 (1975).
3. Measurements of salinity were made with a temperature-compensating Beckman Solubridge that was periodically calibrated against solutions that were prepared from Copenhagen Standard Seawater (chlorinity of 19.373 per mil). Individual determinations were considered accurate to  $\pm 0.2$  per mil.
4. A. J. Gow, S. F. Ackley, W. F. Weeks, J. W. Govoni, *Ann. Glaciol.* 3, 113 (1982); W. F. Weeks and S. F. Ackley, *CRREL Monograph 82-1* (U.S. Army Cold Regions Research and Engineering Laboratory, Hanover, NH, 1982).
5. World Meteorological Organization, *Exec. Comm. Rep.* 8, 107 (1956).
6. W. I. Wittmann and J. J. Schule, *Proceedings of the Symposium on Arctic Heat Budget, Rep. RM-5233-NSF* (Rand Corporation, Santa Monica, CA, 1966).
7. G. A. Maykut, *J. Geophys. Res.* 83, 3646 (1978).
8. G. F. N. Cox and W. F. Weeks, *J. Glaciol.* 13, 109 (1974).
9. D. C. Meeks, G. A. Poe, R. O. Ramseier, *Final Report 1786 FR-1* (Aerojet ElectroSystems Co., Azusa, CA, 1974).
10. W. F. Weeks and A. J. Gow, *J. Geophys. Res.* 83, 5105 (1978); *ibid.* 85, 1137 (1980).
11. This research was sponsored by the U.S. Office of Naval Research through grant N0001484WRM2406. We thank the MIZEX staff and the scientists and crew aboard *Polarstern* for their cooperation during the MIZEX-84 cruise.

19 May 1986; accepted 16 January 1987

## Visualization of Viral Clearance in the Living Animal

ERIC M. VERDIN, ELEFThERIA MARATOS-FLIER,\* C. RONALD KAHN, JEAN-CLAUDE SODOYEZ, FRANCOISE SODOYEZ-GOFFAUX, CLAUDINE J. DE VOS, STEVEN P. LYNN, BERNARD N. FIELDS

The early events in viral dissemination via the bloodstream were identified by monitoring the fate of  $^{125}\text{I}$ -radiolabeled reovirus after it was injected intravenously in rats. Continuous scintillation camera imaging showed that reovirus serotypes 1 and 3 were cleared from the circulation in less than 10 minutes by specific and distinct target organs. Reovirus serotype 1 accumulated predominantly in the lungs and the liver, whereas serotype 3 accumulated in the liver and the spleen with very little virus uptake by the lungs. Incubation of reovirus serotype 1 with a monoclonal antibody directed against the viral hemagglutinin before injection totally inhibited the clearance of the virus by the lungs. Similar results were obtained when viruses biolabeled with  $^{35}\text{S}$  were used. These results demonstrate that viruses can be rapidly transported through the bloodstream to specific target organs and that the localization of the viruses depends on the interaction between specific viral surface components and the target organ.

**A**FTER ENTERING A HOST AND MULTIPLYING at the site of entry, viruses may reach the bloodstream, usually by way of the lymphatic system. Once in the circulation, a virus can potentially localize in any organ of the body within seconds. These early events probably determine the capacity of a virus to reach a target organ distant from the site of entry or to initiate a systemic infection within a host (1). However, the rapidity with which viruses are cleared from the bloodstream and problems inherent to the quantitative recovery of infectious particles from various organs (2) have limited the study of these important early events in a whole animal.

We have used the mammalian reoviruses to analyze how viruses may use the bloodstream to spread within a host. The mammalian reoviruses are small (diameter, 70 nm), icosahedral, nonenveloped viruses containing double-stranded RNA genomes whose

natural hosts include humans, rodents, and bovids (2, 3). Three serotypes, designated 1, 2, and 3, are recognized by their differing neutralization and hemagglutination patterns (4). Genetic studies have enabled the contribution of the individual viral proteins in the pathogenesis of reovirus infection to be defined (5). Protein  $\sigma 1$ , located in the outer capsid of the virus, is responsible for serotype-specific immunologic properties,

E. M. Verdin, E. Maratos-Flier, C. R. Kahn, Research Division, Joslin Diabetes Center, Boston, MA 02215, and Department of Medicine, Brigham and Women's Hospital, Boston, MA 02215.

J.-C. Sodoyez, F. Sodoyez-Goffaux, C. J. De Vos, Department of Internal Medicine and Pediatrics, Hôpital de Bavière, Université de Liège, Liège, Belgium.

S. P. Lynn, Department of Microbiology and Molecular Genetics, Harvard Medical School, Boston, MA 02115. B. N. Fields, Department of Microbiology and Molecular Genetics, Harvard Medical School, and Shipley Institute of Medicine and Department of Medicine, Division of Infectious Disease, Brigham and Women's Hospital, Boston, MA 02115.

\*To whom correspondence should be addressed.

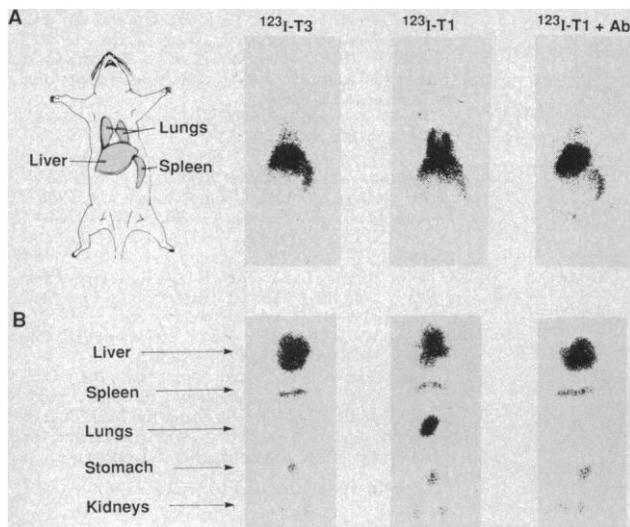


**Fig. 1.** Scintillation scanning image of  $^{123}\text{I}$ -reovirus uptake in vivo. Reovirus serotypes 1 and 3 ( $\sim 100 \mu\text{g}$ ) were iodinated with  $^{123}\text{I}$  ( $\sim 5$  to  $10 \text{ mCi}$  per virus) (Institut National de Radioelements Fleurus, Belgium) by using lactoperoxidase beads (Bio-Rad, Richmond, CA). The reaction was initiated by adding 2% (w/v)  $\beta$ -D-glucose and was allowed to proceed for 10 minutes at room temperature. Labeled virus was then separated from free iodine by chromatography on a G-50 Sephadex column equilibrated with 1% bovine serum albumin in phosphate-buffered saline, pH 7.4. Both viral preparations were used within 4 hours after iodination. Iodinated virus ( $75$  to  $150 \mu\text{Ci}$ , representing  $4 \times 10^7$  to  $8 \times 10^7$  particle-forming units) was injected through a polyethylene catheter into the jugular vein of Sprague-Dawley rats ( $\sim 300 \text{ g}$ ) anesthetized with pentobarbital ( $60 \text{ mg/kg}$  intraperitoneally). Data were collected from the  $128$  by  $128$  pixel matrix of a General Electric 400 Maxi Camera and stored in a Star computer system. (A) Scintigram obtained 5 minutes after the injection of  $^{123}\text{I}$ -labeled serotype 3 ( $^{123}\text{I}$ -T3);  $^{123}\text{I}$ -labeled serotype 1 ( $^{123}\text{I}$ -T1), and  $^{123}\text{I}$ -labeled serotype 1 incubated with an anti- $\sigma 1$  monoclonal antibody before injection (final concentration,  $8 \mu\text{g/ml}$ ). (B) At the end of the 30-minute study, the animals were killed and their organs dissected. A 1-minute static frame was taken of liver, spleen, lungs, stomach, and kidneys.

including neutralization of viral infectivity (6), cytolytic T lymphocyte recognition (7), and delayed-type hypersensitivity response (8, 9). This protein is also the viral hemagglutinin (10), the cell attachment protein (11), and is responsible for distinct cell and tissue tropisms (12).

In order to follow the fate of reovirus serotypes 1 and 3 within a host, we labeled both viruses to a high specific activity with  $^{123}\text{I}$ , an isotope of iodine detectable with a scintillation camera. Adult Sprague-Dawley rats were anesthetized and placed on the high resolution collimator of a scintillation camera. Labeled reovirus was injected intravenously into the jugular vein, and a scintillation image of the whole animal was recorded every 30 seconds during a 30-minute period. We observed that within 5 minutes after the injection, more than 90% of the input of reovirus serotypes 1 and 3 had been cleared from the bloodstream and concentrated in specific organs. Reovirus serotype 1 accumulated in the lungs (mean  $\pm$  SD,  $20 \pm 4\%$  of the amount injected;  $n = 4$ , where  $n$  is the number of animals) and the liver ( $35 \pm 2\%$ ;  $n = 4$ ), whereas reovirus serotype 3 was predominantly cleared by the liver ( $43 \pm 3\%$ ;  $n = 4$ ), and very little virus was sequestered by the lungs ( $4 \pm 2\%$ ,  $n = 4$ ) (Fig. 1). Thus, a total of 55% of reovirus serotype 1 and 47% of serotype 3 was cleared by the liver and the lungs. Uptake of both viruses also occurred in the spleen, but the magnitude of the clearance by this organ could not be quantitated because of superimposition of the stomach, a major site for free iodide clearance (13).

After 30 minutes of study, the animals were killed and their organs were dissected. A 1-minute static frame of the organs removed from the animal confirmed that the liver and the spleen were the major sites of

clearance of reovirus serotype 3. Serotype 1 was found in the liver, spleen, and the lungs (Fig. 1B). The carcass was also examined by scintillation scanning after dissection of these organs and found to contain little residual radioactive material.

To determine the time course of virus uptake by the lungs and liver, we used data accumulated during the 30-minute study (Fig. 2). Uptake of  $^{123}\text{I}$ -labeled viruses by the lungs was rapid, reaching a maximum by 30 seconds after the injection for both serotypes 1 and 3. The amount of labeled reovirus serotype 3 in the lungs rapidly decreased. The initial presence of labeled serotype 3 in the lungs is the result of a large blood pool in that organ, and the subsequent decrease in the amount of labeled virus is due to the equilibration of that blood pool with various organs. The smaller decrease (from 25% to 20%) in the amount of  $^{123}\text{I}$ -labeled serotype 1 represents specific uptake of the virus by lung tissue. The kinetics of accumulation of  $^{123}\text{I}$  in the liver for both serotypes 1 and 3 was different from that observed in the lungs since maximum uptake occurred 10 minutes after the injection (Fig. 2). Ten minutes after the injection of both serotypes, the amount of radioactive material present in the lungs and liver began to decrease linearly with time. This decrease resulted from the partial digestion of the viral outer capsid proteins,  $\mu 1\text{C}$  and  $\sigma 3$ , by these organs after virus uptake. After degradation of the labeled viral proteins, the tracer was released into the bloodstream by the target organs in the form of free iodide or iodotyrosine and subsequently cleared by the stomach and the kidneys (14). These two organs, not visualized during the first 5 minutes after the injection (Fig. 1A), became clearly visible after 30 minutes when significant processing of the viral proteins had taken place (Fig. 1B).

To rule out a possible alteration of the natural properties of the virus during the iodination procedure, we studied the clearance of biosynthetically labeled reovirus serotypes 1 and 3. Viruses were labeled by adding [ $^{35}\text{S}$ ]methionine to the incubation medium during the infectious process. Sprague-Dawley rats received an intravenous injection of purified biolabeled viruses and were killed 20 minutes after the injection. Blood and several organs were processed for measurement of the label. Both viruses were cleared very efficiently from the bloodstream, and reovirus serotype 1 was predominantly taken up by the lungs and the liver whereas reovirus serotype 3 was taken up by the liver and the spleen and very little by the lungs (Fig. 3). These data confirm the results obtained with the  $^{123}\text{I}$ -labeled viruses.

Although humoral immunity plays a critical role in limiting the spread of a viral infection (15), the detailed mechanism of this inhibition is not understood. The presence of antibody on the surface of a viral particle could potentially alter the pattern of clearance. To test this possibility, we incubated reovirus serotype 1 with a monoclonal antibody directed against the  $\sigma 1$  protein (the viral cell attachment protein) and injected both intravenously. Incubation of reovirus serotype 1 with the antibody before injection resulted in a 90% inhibition of lung uptake as compared to the uptake of untreated virus (Figs. 1 and 2). The amount of radioactive material in liver, which was 35% without antibody, increased to 51% in the presence of the antibody (Fig. 2). Similar results were obtained when  $^{35}\text{S}$ -biolabeled reovirus serotype 1 and the monoclonal antibody to  $\sigma 1$  were used. The inhibition of lung uptake was also observed when the Fab fragment of the same antibody was used and demonstrates that the inhibition of

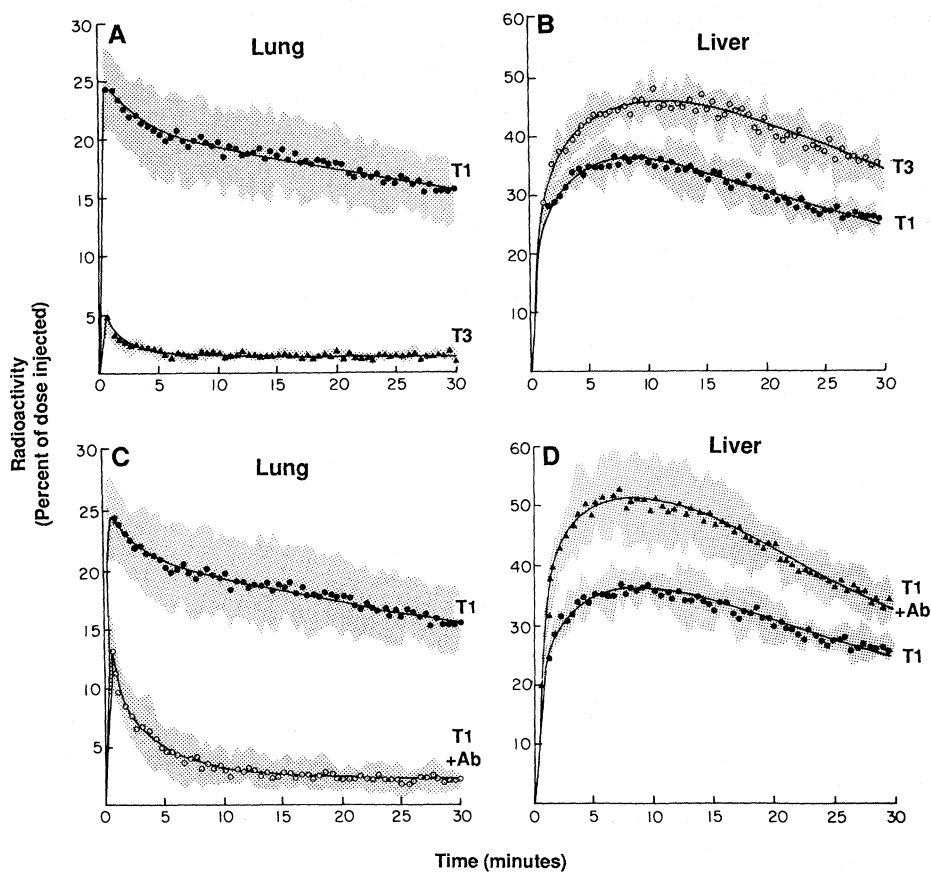


**Fig. 2.** Dynamic scintigram of reovirus serotypes 1 and 3 uptake in vivo. The data generated by the static frame (Fig. 1) were used to recalibrate the data obtained over the 30-minute study by monitoring the radioactive label in small regions of interest defined over specific organs (lungs and liver). (A and B) Time course of (A) lung and (B) liver radioactive isotope content expressed as a percentage of the total dose injected for (●) reovirus serotype 1 (five animals) and (○) serotype 3 (four animals). (C and D) Effect of incubation with the monoclonal antibody to  $\sigma 1$  on (C) lung and (D) liver uptake of (●) serotype 1 (T1) (five animals) and of (▲) serotype 1 plus antibody (four animals). The shaded area represents  $\pm 1$  SD.

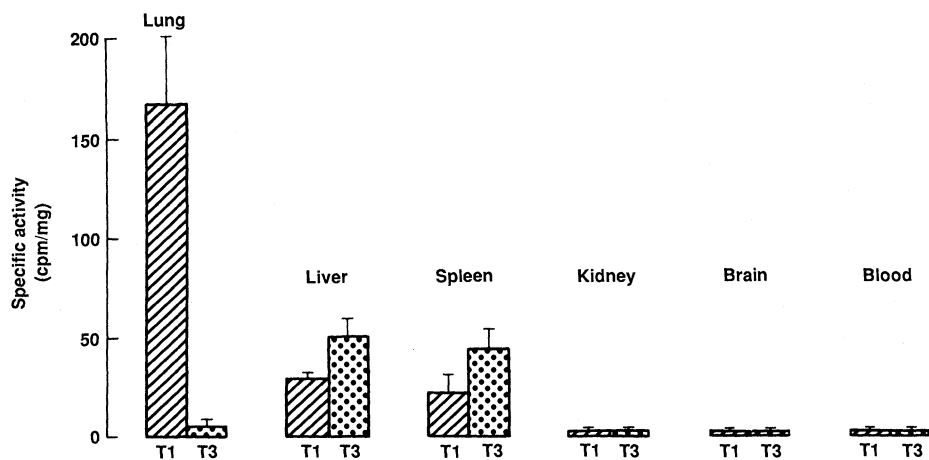


**Fig. 3.** Clearance of  $^{35}\text{S}$ -labeled reovirus type 1 and 3 in vivo. Reovirus serotypes 1 and 3 were grown by infecting L cells in spinner culture. [ $^{35}\text{S}$ ]Methionine (Amersham) was added to the culture medium 8 hours after the initiation of infection and the cells were harvested after 48 to 72 hours. Labeled viruses were purified on a CsCl gradient as previously described (16). The specific activity of these preparations varied from 2.5 to 9 nCi per microgram of protein. Labeled virus was diluted in phosphate-buffered saline and injected into the tail vein of rats under a light ether anesthesia. The rats were killed 20 minutes after injection and their organs were dissected. Approximately 100 mg of tissue from each organ was solubilized at 55°C in Protosol (New England Nuclear), bleached by adding benzoyl peroxide, and counted in a  $\beta$  counter (Rackbeta II, LKB-Produkter, Stockholm, Sweden) after the addition of Aquasol II (New England Nuclear). Results are presented as specific activity in counts per minute per milligram of tissue (mean  $\pm$  SD of six animals) for various organs after the injection of reovirus serotypes 1 (T1) and 3 (T3).

pulmonary clearance can occur independently of viral aggregation. A control monoclonal antibody directed against the  $\sigma 1$  protein of reovirus serotype 3 had no effect on the clearance of either serotype 1 or serotype 3.

These results show the early interaction of a virus in the living host after its entry into the bloodstream. The clearance of reovirus serotypes 1 and 3 is rapid, being completed in less than 10 minutes after the injection of an amount of virus similar to that used in experimental inoculations (3). Despite similar sizes and outer capsid structures, reovirus serotypes 1 and 3 are cleared by different organs after an intravenous injection. Experiments with a monoclonal antibody directed against the viral  $\sigma 1$  protein resulted in the inhibition of uptake of reovirus serotype 1 by the lungs, suggesting that the viral hemagglutinin mediates the pulmonary clearance of reovirus serotype 1. Since the viral hemagglutinin is the cell attachment protein responsible for tissue tropism during a viral infection, the ability of reovirus to localize in the lung may be due to the presence of viral receptors in direct contact with the bloodstream. These experiments demonstrate that an antibody can alter the ability of a virus to use the bloodstream to reach a specific target organ. The inhibition of lung uptake of reovirus serotype 1 by the antibody illustrates a critical defense mechanism against the dissemination of a viral infection within an entire animal.

Instantaneous imaging of organ-specific uptake within a living host was made possible by the radiolabeling of reovirus to a high specific activity and the detection of the radioactive material with a scintillation camera. Using this approach, we have been able to show that viral clearance can be dependent on the interaction between discrete viral components and tissue receptors located in specific organs. Our results suggest that the ability of a virus to be taken up by an organ from the circulation may be an important factor in determining which organ or organs will be involved during the initiation of a viral infection.

#### REFERENCES AND NOTES

1. C. A. Mims and D. O. White, in *Viral Pathogenesis and Immunology* (Blackwell, Palo Alto, CA, ed. 1, 1984), pp. 39–86.
2. W. K. Joklik, Ed., *The Reoviridae* (Plenum, New York, 1983).
3. K. L. Tyler and B. N. Fields, in *Virology*, B. N. Fields, Ed. (Raven, New York, ed. 1, 1985), pp. 823–862.
4. L. Rosen, *Am. J. Hyg.* 71, 242 (1960).
5. A. H. Sharpe and B. N. Fields, *N. Engl. J. Med.* 312, 486 (1985).
6. H. L. Weiner and B. N. Fields, *J. Exp. Med.* 146, 1305 (1977).
7. R. Finberg, H. L. Weiner, B. N. Fields, B. Benacerraf, S. J. Burakoff, *Proc. Natl. Acad. Sci. U.S.A.* 76, 442 (1979).

8. H. L. Weiner, M. I. Greene, B. N. Fields, *J. Immunol.* **125**, 278 (1980).
9. M. I. Greene and H. L. Weiner, *ibid.*, p. 283.
10. H. L. Weiner, R. F. Ramig, T. A. Mustoe, B. N. Fields, *Virology* **86**, 581 (1978).
11. P. W. K. Lee, E. C. Hayes, W. K. Joklik, *ibid.* **108**, 156 (1981).
12. H. L. Weiner, D. Drayna, D. R. Averill, B. N. Fields, *Proc. Natl. Acad. Sci. U.S.A.* **74**, 5744 (1977).
13. J. C. Sodoyez *et al.*, *Science* **219**, 865 (1983).
14. J. C. Sodoyez, F. Sodoyez-Goffaux, Y. M. Morris, *Am. J. Physiol.* **239**, E3 (1980).
15. B. R. Murphy and R. M. Chanock, in *Virology*, B. N. Fields, Ed. (Raven, New York, ed. 1, 1985), pp. 349–370.
16. D. Drayna and B. N. Fields, *J. Gen. Virol.* **63**, 149 (1982).
17. Supported by grants from the National Lottery and Fonds de la Recherche Scientifique Medicale, Brussels, Belgium (to J.C.S. and F.S.G.), a feasibility grant from the American Diabetes Association (to E.M.F.), and by NIH grant AI 3178 (to B.N.F.), and by NIH clinical investigator award AM 01252 (to E.M.F.). We thank M. Okamoto for his expert advice, C. Fallais for the generous supply of  $^{125}\text{I}$ , P. Halban and C. J. Rhodes for reading the manuscript, K. Tyler for helpful discussion of the data, and T.-L. Bellman for excellent secretarial assistance.

29 January 1987; accepted 9 March 1987

## The $\alpha$ Subunit of the GTP Binding Protein $G_k$ Opens Atrial Potassium Channels

JUAN CODINA, ATSUKO YATANI, DAGOBERTO GRENET, ARTHUR M. BROWN, LUTZ BIRNBAUMER

**Guanine nucleotide binding (G) proteins (subunit composition  $\alpha\beta\gamma$ ) dissociate on activation with guanosine triphosphate (GTP) analogs and magnesium to give  $\alpha$ -guanine nucleotide complexes and free  $\beta\gamma$  subunits. Whether the opening of potassium channels by the recently described  $G_k$  in isolated membrane patches from mammalian atrial myocytes was mediated by the  $\alpha_k$  subunit or  $\beta\gamma$  dimer was tested. The  $\alpha_k$  subunit was found to be active, while the  $\beta\gamma$  dimer was inactive in stimulating potassium channel activity. Thus,  $G_k$  resembles  $G_s$ , the stimulatory regulatory component of adenylyl cyclase, and transducin, the regulatory component of the visual system, in that it regulates its effector function—the activity of the ligand-gated potassium channel—through its guanine nucleotide binding subunit.**

**R**ECENT WORK (1, 2) DEMONSTRATED that a heterotrimeric pertussis toxin (PTX)-sensitive guanine nucleotide binding (G) protein, purified from human red blood cells (hRBC) and treated with guanosine ( $\gamma$ -thio)triphosphate (GTP $\gamma$ S) and magnesium, causes opening of a subset of potassium channels present in isolated membrane patches of atrial cells from adult guinea pig hearts and pituitary GH $_3$  tumor cells. The properties of these channels are similar to those activated in these cells by receptor ligands such as acetylcholine (ACh), acting through muscarinic receptors (mAChR), and somatostatin, acting through its separate specific receptors. The channels are also opened by GTP $\gamma$ S and Mg $^{2+}$ , which presumably act by stimulating a G protein endogenous to the cardiac membrane patch. Based on its activity, we called this G protein  $G_k$  (3).

The response to receptor ligands is guanosine triphosphate (GTP)-dependent and abolished by PTX, and, after PTX treatment, is restored by addition of untreated  $G_k$  from hRBC in the presence of GTP. Thus, ligand-induced opening of K $^+$  channels in isolated membrane patches is controlled in a manner analogous to hormonal stimulation of adenylyl cyclases;  $G_k$  activation is GTP-dependent and stimulated by occupied receptors,

and K $^+$  channels are the effectors "sensing" the activity state of  $G_k$ .

In our experiments (1, 2), opening of K $^+$  channels was specific for the PTX-sensitive G protein of hRBC and occurred at picomolar concentrations.  $G_s$  at nanomolar concentrations was unable to substitute for  $G_k$  either in coupling receptors to the K $^+$  channel in the presence of GTP or, after treatment with GTP $\gamma$ S and Mg $^{2+}$ , in directly causing K $^+$  channel opening.

It is commonly thought that activation of G proteins involves tight binding of the guanine nucleotide (a Mg $^{2+}$ -dependent step) and dissociation of the heterotrimer into an activated  $\alpha$ -G nucleotide complex plus free  $\beta\gamma$ . The purified  $\alpha_s$ -GTP $\gamma$ S complex is sufficient for stimulation of adenylyl cyclase (4). For inhibition of adenylyl cyclase, the situation is more complex because, even though resolved  $\alpha_i$ -GTP $\gamma$ S complexes purified from liver were shown to inhibit enzyme activity by Katada *et al.* (5),  $\beta\gamma$  dimers also inhibited adenylyl cyclase and did so at lower concentrations. Although they did not discount a role for  $\alpha_i$ , these authors proposed that  $\beta\gamma$  dimers may account for a major proportion of G $_i$ -mediated inhibition of adenylyl cyclase (5).

Human erythrocyte  $G_k$ , with which we stimulated K $^+$  channels and reconstituted

receptors coupling to K $^+$  channels after treatment with PTX, is also formed of  $\alpha\beta\gamma$  subunits and dissociates into  $\alpha$ -GTP $\gamma$ S plus  $\beta\gamma$  under the conditions used for activation and testing of its activity (6). Because GTP $\gamma$ S-treated  $G_s$ , a mixture of  $\alpha_s$ -GTP $\gamma$ S plus  $\beta\gamma$  subunits that are biochemically indistinguishable from those present in the human erythrocyte  $G_k$  (7), did not stimulate K $^+$  channels, it seemed that the  $\alpha$  subunit and not the  $\beta\gamma$  dimer was responsible for the effect of  $G_k$  and K $^+$  channels.

Unexpectedly, however, Logothetis *et al.* (8) reported opening of atrial K $^+$  channels in isolated membrane patches from embryonic chick atria to be caused by  $\beta\gamma$  complexes and not by  $\alpha$  subunits purified from bovine brain (9, 10). The bovine brain  $\beta\gamma$  preparations had previously been shown by two-dimensional tryptic peptide mapping to be indistinguishable from human erythrocyte  $\beta\gamma$  dimers (7).

In light of these conflicting results, we reexamined the validity of our inferred conclusion that  $\alpha_k$ , rather than  $\beta\gamma$  from  $G_k$ , caused the K $^+$  channel opening we had observed. We prepared  $\beta\gamma$  complexes, resolved as well as possible from PTX-sensitive  $\alpha$  subunits, and  $\alpha_k$ -GTP $\gamma$ S complexes, resolved as well as possible from  $\beta\gamma$  subunits (Fig. 1), and tested their individual effects on guinea pig atrial K $^+$  channels as described (1).

Ion exchange chromatography (11) was used to obtain  $\alpha_k$ -GTP $\gamma$ S ( $\alpha_k^*$ ) from GTP $\gamma$ S-activated human erythrocyte  $G_k$  ( $G_k^*$ ). The resulting preparation was analyzed by SDS-polyacrylamide gel electrophoresis followed by densitometry of the gel after staining first with Coomassie blue and then with silver; the standards were increasing amounts of bovine serum albumin ranging from 0.001 to 10  $\mu$ g per lane. We obtained a solution that contained 36  $\mu$ g of  $\alpha_k^*$  per milliliter and 0.4  $\mu$ g of  $\beta\gamma$  per milliliter, to which we ascribed a nominal concentration of 1  $\mu$ M  $\alpha_k^*$  and 0.01  $\mu$ M  $\beta\gamma$  (estimation error,  $\pm 10\%$ ). The Coomassie blue-stained polyacrylamide gel onto which 2  $\mu$ g of the starting hRBC  $G_k$  and 0.5  $\mu$ g of the resulting hRBC  $\alpha_k^*$  had been applied is shown in Fig. 1. The method used to prepare  $\alpha_k^*$  did not yield significant amounts of free  $\beta\gamma$  subunits. These were prepared separately from human erythrocytes (Fig. 1) and bovine brain (Fig. 1) with methods that do not involve stabilization with activating

J. Codina and D. Grenet, Department of Cell Biology, Baylor College of Medicine, Houston, TX 77030.

A. Yatani and A. M. Brown, Department of Physiology and Molecular Biophysics, Baylor College of Medicine, Houston, TX 77030.

L. Birnbaumer, Department of Cell Biology and Department of Physiology and Molecular Biophysics, Baylor College of Medicine, Houston, TX 77030.